

# Prediction of Interpolants in Zero Diluted Images

T. Kishan Rao, M. Shankar Lingam, Manish Prateek, and E. G. Rajan

**Abstract** — This paper provides an algorithmic procedure to predict interpolants of zero diluted images. Given a digital image, one can zero dilute it by right adjoining a column consisting of ‘0s’ to every column except the last column and inserting a row consisting of ‘0s’ below every row except the last row. This yields a new image with a size  $(2W-1) \times (2H-1)$ , where  $W$  is the width and  $H$  is the height of the original image. Another way of zero diluting an image is by right adjoining a column consisting of ‘0s’ to every column and inserting a row consisting of ‘0s’ below every row. This yields a new image with a size  $(2W) \times (2H)$ , where  $W$  is the width and  $H$  is the height of the original image. Alternatively, subsampling of an image is carried out by forcing pixel values in the alternate columns and rows to zero. Thus, the size of the subsampled image is reduced to half of the size of the original image. This means 75% of the information in the original image is lost in the subsampled image. On the other hand, zero dilution of an image does not cause loss of information but increases the possibility of predicting more information. The question that arises here is whether it is possible to predict more pixel values, which are called interpolants so that the reconstructed image is an enhanced version of the original image in resolution. In this paper, two novel interpolant prediction techniques, which are reliable and computationally efficient, are discussed. They are (i) interpolant prediction using neighborhood pixel value averaging and (ii) interpolant prediction using extended morphological filtering. These techniques can be applied to predict interpolants in a subsampled image also.

**Index Terms** — Ground Penetrating Radar, Zero Diluted Imaging, Targeted Buried Object Detection, Interpolant Prediction.

## I. INTRODUCTION

**Digital zoom-in** increases the size of the pixels leaving a pixelated image that often is not even suitable for viewing on screen. Resizing of an image also causes similar kind of pixelation problem. Alternatively, one can enlarge a given image using the technique described below.

### A. Concept of Zero Dilution

Fig. 1 shows an array of size  $9 \times 9$  and its zero diluted version of size  $17 \times 17$ . One can also zero dilute the  $9 \times 9$  array by adding one column at the right and one more row at the bottom of the array so that one gets zero diluted array

of size  $18 \times 18$ , which is the double the size of given array. Depending on requirement, one may choose either of the methods.

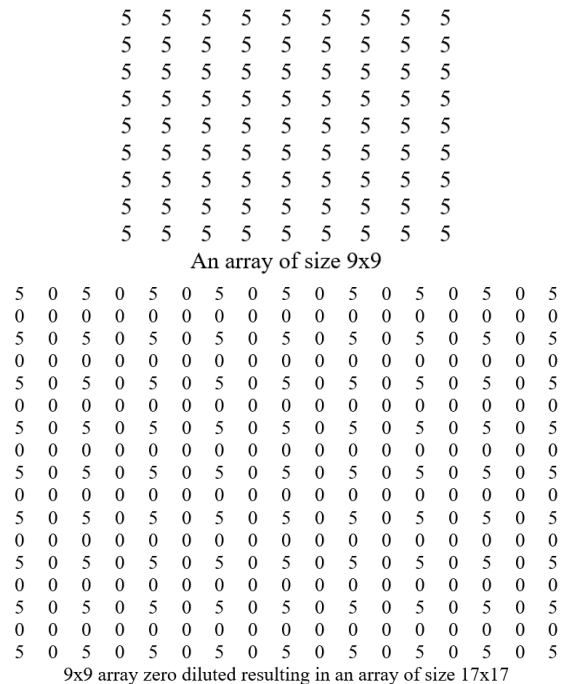


Fig. 1. An array of size  $9 \times 9$  and its zero diluted form.

Fig. 2 shows a sample gold mine image of size  $1177 \times 891$  and its zero diluted version of size  $2353 \times 1781$ . This is achieved using the technique demonstrated in Fig. 1. The 0’s are called the ‘interpolants’. The question that arises here is whether it is possible to predict suitable values for the interpolants so that the enlarged image does not show up pixelation effects. In this paper, two techniques of (i) interpolant prediction using neighborhood pixel value averaging and (ii) interpolant prediction using extended morphological filtering are briefly explained. Consider the sample gold mine image of size  $1177 \times 891$  shown in Fig. 1. After applying the zero dilution algorithm to this image, one gets the zero diluted image of size  $2353 \times 1781$ , which is also shown in Fig. 1.



Gold mine image (Size =  $1177 \times 891$ )

Published on January 12, 2021.  
T. Kishan Rao, Research Scholar, MG-NIRSA, University of Mysore, India.  
(e-mail: kishanrao65@gmail.com)  
Dr. M. Shankar Lingam, Research Associate, NIRDPR, Hyderabad, India.  
(e-mail: shankumacharla@gmail.com)  
Manish Prateek, Professor and Dean, University of Petroleum & Energy Studies, Dehradun, Uttarakhand, India.  
(e-mail: mprateek@ddn.upes.ac.in)  
E. G. Rajan, Adjunct Professor, Department of Cybernetics, University of Petroleum and Energy Studies, Dehradun, Hon. Director MG-NIRSA, NIRSA, Hyderabad, India.  
(e-mail: dr.rajaneg@gmail.com)



Gold mine image zero diluted.  
(Size = 2353×1781)

Fig. 2. A sample gold mine image and its zero diluted form.

In what follows, the image reconstruction is carried out using the two interpolant predicting techniques mentioned above.

## II. INTERPOLANT PREDICTION TECHNIQUES

### A. Interpolant Prediction Using Neighborhood Pixel Value Averaging

This is a computationally intensive process for interpolant prediction.

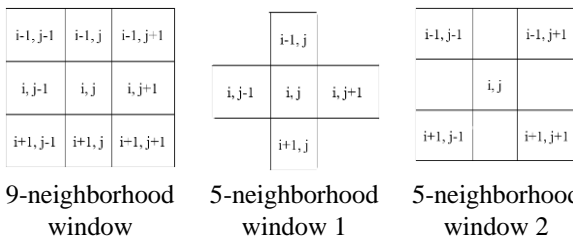
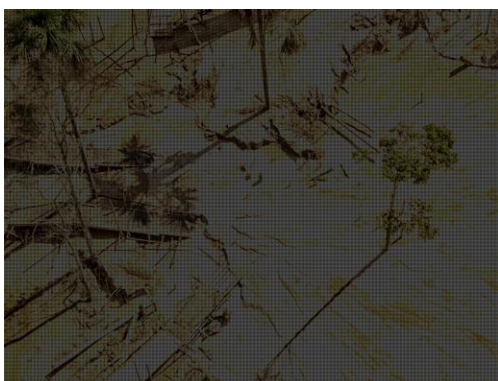


Fig. 3. Basic scanning windows used in image processing.

Scan the subsampled image with the 9-neighborhood window shown in Fig. 3. At every position, the interpolant is evaluated as the average of all available non-zero values using the prediction formula.

$$\frac{x(i-1, j-1)+x(i-1, j)+x(i-1, j+1)+x(i, j-1)+x(i, j)+x(i, j+1)+x(i+1, j-1)+x(i+1, j)+x(i+1, j+1)}{n}$$

where n is the number of non-zero pixel values. The algorithm is applied to the whole image. Fig. 4 shows the sample gold mine image zero diluted and its pixel averaged version.



Gold mine image zero diluted  
(Size = 2353×1781)



Reconstructed image using pixel averaging.  
(Size = 2353×1781)

Fig. 4. A sample gold mine image zero diluted and its pixel averaged version.

### B. Interpolant Prediction Using Extended Morphological Filtering

Morphological filtering makes use of two fundamental operations of ‘dilation’ and ‘erosion’, which are defined as follows. **Dilation:** Let image to be dilated be A and the structuring element that dilates A be B. Then the dilation of A by B is defined as the Minkowski addition  $D(A,B) = A \oplus B = \text{EXTSUP}_{(x,y) \in D_B} [A_{x,y} + B(x,y)]$ , where  $D_B$  is the domain of the image B, and EXT SUP is an operation of supremum over the union of the domains. **Erosion:** Let image to be eroded be A and the structuring element that erodes A be B. Then the erosion of A by B is defined as the Minkowski subtraction  $A \ominus B = \text{INF}_{(x,y) \in D_B} [A_{x,y} - B(x,y)]$  as  $E(A,B) = \text{INF}_{(x,y) \in D_B} [A_{x,y} - B(x,y)]$ , where  $D_B$  is the domain of the image B, and INF is an operation of infimum over the intersection of the domains. Following these definitions, morphological filtering operations of **Closing** and **Opening** are defined in the following manner. Closing of A by B is represented as  $A \circ B$  and defined as  $A \circ B = (A \oplus B) \ominus B$ . Opening of A by B is represented as  $A \bullet B$  and defined as  $A \bullet B = (A \ominus B) \oplus B$ . Same structuring element should be used for dilation and erosion in any morphological filtering. Now,  $(A \circ B) \circ (A \circ B) = A \circ B$  and  $(A \bullet B) \bullet (A \bullet B) = A \bullet B$ , which means closing and opening are idempotent operators.

#### 1. Extended morphological filters

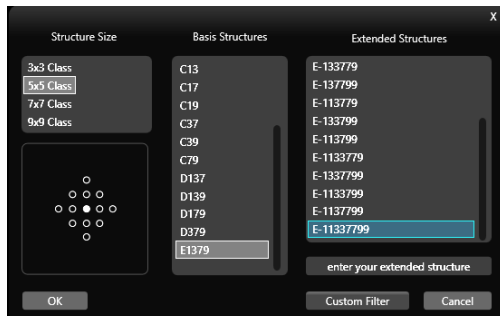
These are essentially morphological filters except that the structuring element need not remain the same for dilation and erosion in any morphological filtering. With reference to Fig. 5, for example, one can use the structuring element E11337799 for dilation and subsequently E1379 for erosion, so that extended closing operation is carried out on a given image. The structuring elements of E11337799 and E1379 are shown in the respective dialog boxes. Extended morphological filtering is a computationally less intensive process for interpolant prediction. At every position, the interpolant is evaluated using the procedure given below. Scan the given subsampled image and dilate it with E-11337799 shown in Fig. 5. Subsequently, erode with E-1379 shown in Fig. 5. The resulting image is extended morphological filtered version, which is also the interpolant predicted version. By extended morphological filtering, one can reconstruct the original image from the subsampled version, which means the lost information is predicted. Let us take some sample images and do the process of

subsampling and extended morphological filtering. Fig. 8 shows a sample image of a gold mine, its subsampled version, the subsampled image dilated using structuring element E-11337799 and the dilated image eroded again using structuring element E-1379. Scan subsampled image with E-11337799. At every position, find the maximum image pixel value and assign it to the central pixel and thus dilation is carried out. Then, scan dilated version of subsampled image with E-1379. At every position, find the minimum image pixel value and assign it to the central pixel and thus erosion is carried out.

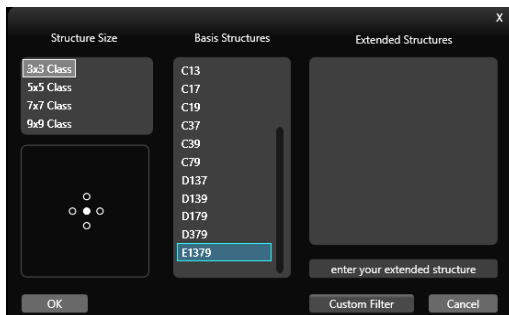


Reconstructed image using extended morphological filter.  
(Size = 2353×1781)

Fig. 6. A sample gold mine image zero diluted and its extended morphological filtered version.



Neighborhood structure E-11337799

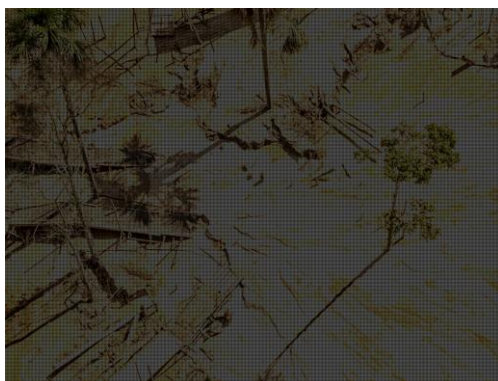


Neighborhood structure E-1379

Fig. 5. Structuring elements used for extended morphological filtering.

### 2. Information gain due to zero dilation and reconstruction using extended morphological filtering

Given an image of size 100×100, size of its zero diluted version turns out to be 199×199. The number of pixels in the zero diluted version is 39,601, whereas number of pixels in the original image is 10,000. This means 396.01% additional predicted information is added to the original image by zero diluting it followed by extended morphological filtering.



Gold mine image zero diluted.  
(Size = 2353×1781)

### 3. Comparative study of prediction using neighborhood pixel value averaging and extended morphological filtering

A comparative study is made on the two interpolant prediction techniques in terms of visual quality analysis. Visual quality parameters include Trade of Threshold (ToT), entropy and visual quality. ‘Statistical parameters’ is also another measure by which one can compare the two techniques. However, due to space restriction, this paper provides results of comparative study based on visual quality parameters only.

#### C. Visual Quality Parameters of Gold Mine Image, Its Subsamped Image, and Reconstructed Images Using Prediction Formula and Extended Morphological Filter

Visual quality increases as one decreases the entropy of an image. The entropy of an image refers to the degree of randomness in the given image. Noise adds to entropy but reduces visual quality and filtering reduces entropy but increases visual quality. For better visual quality and considerable entropy, one has to accept a trade-off between the two. Visual quality is generally improved by quantizing an image with a threshold value (Th). The number of segments in an image depends on threshold value (Th). More the threshold value, less the number of segmented regions in an image. Less the number of segments, more is the visual quality. The visual quality parametric values of the original gold mine image, its zero diluted and the reconstructed images using extended morphological filter are presented in Table 1.

TABLE I: VISUAL QUALITY PARAMETERS OF THE ORIGINAL GOLD MINE IMAGE, ITS ZERO DILUTED IMAGE AND THE RECONSTRUCTED IMAGES USING PIXEL AVERAGING AND EXTENDED MORPHOLOGICAL FILTERING METHODS

Gold mine image (Size = 1177×891)			Gold mine image zero diluted (Size = 2353×1781)		
Th	Visual Quality	Entropy	Th	Visual Quality	Entropy
0	0	100	0	0.004390682	99.99560932
1	0	100	1	0.004390682	99.99560932
2	0.001239622	99.99876038	2	0.004390682	99.99560932
3	0.008200575	99.99179943	3	0.017371828	99.98262817
4	0.029464855	99.97053514	4	0.017371828	99.98262817
5	0.072756261	99.92724374	5	0.017371828	99.98262817
6	0.177838042	99.82216196	6	0.041496717	99.95850328
7	0.327164785	99.67283522	7	0.041496717	99.95850328
8	0.586150374	99.41384963	8	0.041496717	99.95850328
9	0.957274053	99.04272595	9	0.081060579	99.91893942
10	1.440345111	98.55965489	10	0.081060579	99.91893942

11	2.053862518	97.94613748	11	0.081060579	99.91893942	91	89.08408164	10.91591836	91	14.72073951	85.27926049
12	2.805359362	97.19464064	12	0.125325334	99.87467467	92	89.46931793	10.53068207	92	15.2112789	84.7887211
13	3.682439423	96.31756058	13	0.125325334	99.87467467	93	89.83119213	10.16888077	93	15.27551648	84.72448352
14	4.649249028	95.35075097	14	0.125325334	99.87467467	94	90.18858461	9.811415391	94	15.54792966	84.45207034
15	5.770629928	94.22937007	15	0.215835424	99.78416458	95	90.5391115	9.460888504	95	15.82136892	84.17863108
16	7.00348143	92.99651857	16	0.215835424	99.78416458	96	90.87018586	9.129814143	96	16.09845913	83.90154087
17	8.373358812	91.62664119	17	0.33949039	99.66050961	97	91.20545586	8.794544139	97	16.36729295	83.63270705
18	9.775180293	90.22481971	18	0.33949039	99.66050961	98	91.52594576	8.47405424	98	16.64070835	83.35929165
19	11.28952129	88.71047871	19	0.395495447	99.60450455	99	91.82889024	8.171109757	99	16.91803718	83.08196282
20	12.85478213	87.14521787	20	0.395495447	99.60450455	100	92.13107188	7.868928118	100	17.2900043	82.7099957
21	14.48984321	85.51015679	21	0.514735868	99.48526413	101	92.41685237	7.583147628	101	17.45544233	82.54455767
22	16.13958904	83.86041096	22	0.514735868	99.48526413	102	92.70015362	7.299846382	102	17.73405974	82.26594026
23	17.83548694	82.16451306	23	0.645835904	99.3541641	103	92.97353789	7.02646211	103	18.01134085	81.98865915
24	19.53281517	80.46718483	24	0.645835904	99.3541641	104	93.2395381	6.766046188	104	18.29547046	81.70452954
25	21.27229054	78.72770946	25	0.732718908	99.26728109	105	93.49589542	6.504104578	105	18.58306013	81.41693987
26	23.0218736	76.9781264	26	0.912856179	99.08714382	106	93.74906432	6.250935676	106	18.86418308	81.13581692
27	24.78490179	75.21509821	27	0.912856179	99.08714382	107	93.98325748	6.016742522	107	19.16141316	80.83585864
28	26.49453088	73.50546912	28	1.008448961	98.99155104	108	94.22851187	5.771488128	108	19.46017043	80.53982957
29	28.23267128	71.76732872	29	1.213331542	98.78666846	109	94.45450445	5.545495548	109	19.75525289	80.24474711
30	29.98625927	70.01374073	30	1.213331542	98.78666846	110	94.66323768	5.336762318	110	20.0502399	79.9497601
31	31.70494714	68.29505286	31	1.328300594	98.67169941	111	94.87874115	5.121258845	111	20.35248108	79.64751892
32	33.45414878	66.5458122	32	1.445417262	98.5548274	112	95.0755495	4.924445055	112	20.65438819	79.34581181
33	35.0942637	64.9057363	33	1.570838045	98.42916195	113	95.27475262	4.725247376	113	20.95481583	79.04518417
34	36.7910198	63.2089802	34	1.696258829	98.30374117	114	95.46040982	4.539590181	114	21.26431118	78.73568882
35	38.39613925	61.60386075	35	1.696258829	98.30374117	115	95.63929677	4.360703228	115	21.57841197	78.42158803
36	40.02280904	59.97719096	36	1.966238042	98.03367196	116	95.82180724	4.178192765	116	21.89081854	78.10918146
37	41.6609215	58.3390785	37	2.119267625	97.88073238	117	95.99077721	4.009222786	117	22.21551424	77.78448576
38	43.17316467	56.82683533	38	2.27232107	97.72767893	118	96.15869828	3.841301717	118	22.53958951	77.46041049
39	44.70037866	55.29962134	39	2.427856204	97.5721438	119	96.32366333	3.67633667	119	22.87519033	77.12480967
40	46.21243112	53.78756888	40	2.582389118	97.41761088	120	96.47403898	3.525961017	120	23.20988438	76.79011562
41	47.67537549	52.32462451	41	2.743126256	97.25687374	121	96.6142116	3.385788404	121	23.50580308	76.44916962
42	49.10008229	50.89991771	42	2.911117565	97.08888244	122	96.75047463	3.249525368	122	23.8934706	76.1065294
43	50.58924943	49.41075057	43	3.086148281	96.91385172	123	96.88416307	3.115836931	123	24.24885335	75.75114665
44	51.93709969	48.06290031	44	3.25523726	96.74476274	124	97.01747008	2.982529915	124	24.62225221	75.37774779
45	53.28237534	46.71762466	45	3.442246903	96.5577531	125	97.14629539	2.85370461	125	25.00118715	74.99881285
46	54.60505174	45.39494826	46	3.455967784	96.54403222	126	97.26672941	2.733270589	126	25.38055162	74.61944838
47	55.89912149	44.10087851	47	3.821802265	96.17819773	127	97.38363528	2.616364723	127	25.77053485	74.22946515
48	57.13874323	42.86125677	48	4.010697037	95.98930296	128	97.49129166	2.508708343	128	26.16614961	73.83385039
49	58.38208384	41.61791616	49	4.212143433	95.78785657	129	97.59961553	2.400384473	129	26.57541366	73.42458634
50	59.60168093	40.39831907	50	4.415832894	95.58416711	130	97.69725958	2.302740422	130	26.97374873	73.02625127
51	60.75872479	39.24127521	51	4.611576176	95.38842382	131	97.79128012	2.208719881	131	27.3986188	72.6013812
52	61.89803253	38.10196747	52	4.830370538	95.16962946	132	97.88396568	2.116034317	132	27.81697442	72.18302558
53	63.03037931	36.96962069	53	5.040311948	94.95968805	133	97.97236025	2.027639751	133	28.25749822	71.74250178
54	64.07662007	35.92337993	54	5.040311948	94.95968805	134	98.05466382	1.943536183	134	28.69585054	71.30414946
55	65.12133513	34.87866487	55	5.472985017	94.52701498	135	98.13513212	1.86486788	135	29.14355692	70.85644308
56	66.18397703	33.81602297	56	5.695406464	94.30459354	136	98.20922336	1.790776642	136	29.60536599	70.39463401
57	67.16585281	32.83414719	57	5.705929783	94.29407022	137	98.28560313	1.714396872	137	30.07793699	69.92206301
58	68.14744252	31.85255748	58	6.160055151	93.85894485	138	98.35387768	1.64612232	138	30.566867	69.4333133
59	69.11081932	30.88918068	59	6.160055151	93.83994485	139	98.42358256	1.576417436	139	31.06285762	68.93714238
60	70.04034492	29.95965508	60	6.637255461	93.36274454	140	98.48556365	1.514436349	140	31.5790491	68.4209509
61	70.93630537	29.06369463	61	6.637255461	93.36274454	141	98.54678189	1.453218106	141	32.10103914	67.89896086
62	71.83922678	28.16077322	62	7.119514601	92.8804854	142	98.60237416	1.397625838	142	32.6348172	67.3651828
63	72.70133603	27.29866397	63	7.377156952	92.62284305	143	98.65501041	1.344989592	143	33.17544378	66.82455622
64	73.52921264	26.47078736	64	7.377156952	92.62284305	144	98.70116248	1.298837521	144	33.73074573	66.26925427
65	74.36366878	25.63633122	65	7.889888379	92.11011162	145	98.75236839	1.247631607	145	34.30857378	65.69142622
66	75.14443977	24.85556023	66	7.890341764	92.10965824	146	98.8009971	1.199000293	146	34.88652116	65.11347884
67	75.90451861	24.09548139	67	8.151324852	91.84867515	147	98.84734249	1.152657511	147	35.49983261	64.50016739
68	76.65649223	23.34350777	68	8.681809906	91.31819009	148	98.88882214	1.11117786	148	36.12509912	63.87490088
69	77.40427021	22.59572979	69	8.945608757	91.05439124	149	98.92658293	1.073417075	149	36.75446996	63.24553004
70	78.07957799	21.92042201	70	8.945608757	91.05439124	150	98.96558333	1.034416667	150	37.37842405	62.62157595
71	78.79522116	21.20477884	71	9.211101839	90.78889816	151	99.00115094	0.998849059	151	38.02542921	61.97453709
72	79.44478296	20.55521704	72	9.482035549	90.51796445	152	99.03633713	0.963662872	152	38.68734837	61.31265163
73	80.10397566	19.89602434	73	9.749318311	90.25068169	153	99.06847194	0.931528063	153	39.34697674	60.65302326
74	80.72140264	19.27859736	74	10.02347344	89.97652656	154	99.0981275	0.901872496	154	40.02836762	59.97163238
75	81.34235778	18.65764222	75	10.30273513	89.69726487	155	99.12959482	0.870405175	155	40.71414919	59.28585081
76	81.92574284	18.07425716	76	10.58514666	89.41485334	156	99.15877361	0.841226386	156	41.39570711	58.60429289
77	82.51036753	17.48963247	77	10.85639058	89.14360942	157	99.18509174	0.814908263	157	42.09091432	57.90908568
78	83.06514594	16.93485406	78	11.13546137	88.86453863	158	99.21322161	0.786778385	158	42.79798115	57.20201885
79	83.61191448	16.38808552	79	11.41283792	88.58716208	159	99.23114845	0.768851548	159	43.49218614	56.50781386
80	84.14418899	15.85581101	80	11.69639484	88.30360516	160	99.25603344	0.747396556	160	44.19056705	55.80943295
81	84.67674956	15.32325044	81	11.96740014	88.03259986	161	99.27339095	0.726609053	161	44.91228539	55.08771461
82	85.15533891	14.84466109	82	12.23616237	87.76383763	162	99.29074565	0.709254348	162	45.63464802	54.36535198
83	85.65404827	14.34595173	83	12.50840851	87.49159149	163	99.30733751	0.692662488	163	46.35269155	53.64730845
84	86.12596273	13.84503727	84	12.77709916	87.22290084	164	99.32331326	0.67368674	164	47.07684385	52.92315615
85	86.58538562	13.41461438	85	13.06130036	86.93869964	165	99.34385868	0.656141325	165	47.80722425	52.19277575
86	87.03555903	12.96444097	86	13.33893941	86.66106059	166	99.35873414	0.641265864	166		



68	95.40424542	4.595754582	68	92.2738077	7.726192303	148	99.4799931	0.520068999	148	99.51747837	0.482521626
69	95.66151461	4.338485392	69	92.61573205	7.384267948	149	99.48193347	0.518066533	149	99.52370646	0.476293539
70	95.9084854	4.091514598	70	92.92582396	7.074176037	150	99.48469878	0.515301223	150	99.52993455	0.470066542
71	96.14048538	3.859514621	71	93.24407681	6.755923185	151	99.48822693	0.511773069	151	99.53513655	0.464863449
72	96.35894487	3.641055128	72	93.53538902	6.464610984	152	99.49309006	0.506909938	152	99.53986131	0.462438693
73	96.56643848	3.433561519	73	93.83008968	6.169910323	153	99.49585537	0.504144628	153	99.54542125	0.454578753
74	96.77212033	3.227879665	74	94.10097566	5.899024338	154	99.49871604	0.501283962	154	99.55081415	0.449185851
75	96.95424938	3.045750624	75	94.36546652	5.634533477	155	99.5015767	0.498423296	155	99.55501393	0.444986068
76	97.12636609	2.873633913	76	94.61427979	5.385720214	156	99.50462808	0.49537192	156	99.56052615	0.439473853
77	97.28923331	2.710766687	77	94.85715131	5.142848689	157	99.5075841	0.492415899	157	99.56513159	0.43486841
78	97.44075323	2.559246768	78	95.08241238	4.917587616	158	99.51025406	0.489745944	158	99.5693791	0.430620902
79	97.58340509	2.416594912	79	95.30268621	4.697313786	159	99.51263794	0.487362056	159	99.57360274	0.426397257
80	97.72348235	2.276517655	80	95.51401164	4.485988356	160	99.51511719	0.484882813	160	99.57818432	0.421815676
81	97.85259372	2.147406282	81	95.72383374	4.276166257	161	99.51759643	0.482403569	161	99.58221707	0.41778293
82	97.97445807	2.025541929	82	95.9128001	4.087199897	162	99.51998032	0.480019681	162	99.58624982	0.413750184
83	98.08850327	1.911496729	83	96.09603949	3.903960514	163	99.52341312	0.476586883	163	99.59023484	0.409765163
84	98.1986389	1.801361105	84	96.27171449	3.728285513	164	99.52541558	0.474584417	164	99.59410055	0.405899454
85	98.2972365	1.702763498	85	96.43858426	3.561415737	165	99.52789483	0.472105173	165	99.59756059	0.402439406
86	98.38267505	1.617324953	86	96.59784193	3.402158068	166	99.52951587	0.47048413	166	99.60133085	0.398669146
87	98.4700207	1.529979298	87	96.75631214	3.243687858	167	99.53151834	0.468481664	167	99.60438524	0.395614759
88	98.54477943	1.455220572	88	96.90444993	3.095550068	168	99.53361616	0.466383842	168	99.60698624	0.393013757
89	98.61887067	1.381129334	89	97.05110825	2.948891747	169	99.5353256	0.464667443	169	99.61123375	0.388766249
90	98.68600095	1.313999048	90	97.18538199	2.814618012	170	99.53762109	0.46237891	170	99.61466994	0.385330064
91	98.74922166	1.250778339	91	97.30681775	2.693182249	171	99.53914678	0.460853222	171	99.61774819	0.382251814
92	98.80624426	1.193755739	92	97.43252488	2.567475117	172	99.54153067	0.458469334	172	99.62058781	0.379412188
93	98.85506629	1.144933714	93	97.54245897	2.457451102	173	99.54267493	0.457325068	173	99.62302178	0.376978223
94	98.90789324	1.092106756	94	97.65067496	2.34932504	174	99.54563095	0.454369047	174	99.62627606	0.373732936
95	98.95480816	1.045191841	95	97.75497752	2.245022482	175	99.54782413	0.45217587	175	99.62889193	0.371108072
96	98.99581103	1.004188968	96	97.85493712	2.145062881	176	99.54944517	0.450554826	176	99.63187473	0.368125272
97	99.03280897	0.967191027	97	97.9481198	2.051880202	177	99.551543	0.448457005	177	99.63616996	0.36383004
98	99.06828123	0.931718774	98	98.03688793	1.963112068	178	99.55306868	0.446931316	178	99.63819826	0.361801735
99	99.10299064	0.897009365	99	98.12286417	1.877135834	179	99.55554793	0.444452073	179	99.64158673	0.358413274
100	99.13340905	0.866590954	100	98.20189644	1.798103559	180	99.5577411	0.442258896	180	99.64442635	0.355573649
101	99.16010859	0.839891409	101	98.27751639	1.722483608	181	99.56012499	0.439875008	181	99.64831592	0.351684077
102	99.18776169	0.812238309	102	98.34903201	1.65096799	182	99.56231817	0.437681831	182	99.65258729	0.347412707
103	99.21417517	0.78582483	103	98.41718303	1.582816971	183	99.56622775	0.433772255	183	99.65547464	0.344525357
104	99.23686978	0.763130217	104	98.4822558	1.517744201	184	99.56794414	0.432055855	184	99.65900628	0.340993721
105	99.25803871	0.741961291	105	98.5424845	1.457515499	185	99.57099552	0.429004479	185	99.66170273	0.33829727
106	99.27577484	0.724225165	106	98.60202119	1.397978807	186	99.57442832	0.42557168	186	99.66459008	0.335409919
107	99.2906503	0.709349704	107	98.65781149	1.342188512	187	99.57500045	0.424999547	187	99.6681933	0.331806696
108	99.30829107	0.691708933	108	98.71112009	1.288879906	188	99.57652614	0.423473859	188	99.67122383	0.328776171
109	99.3217362	0.678263805	109	98.7616368	1.238363202	189	99.57728899	0.422711015	189	99.67425435	0.325745646
110	99.33336957	0.666630432	110	98.80781055	1.192189454	190	99.57881467	0.421185326	190	99.67726102	0.322738984
111	99.34385868	0.656141325	111	98.85350705	1.146492955	191	99.5800543	0.419945705	191	99.6806972	0.319302798
112	99.35482456	0.64517544	112	98.8955526	1.104447403	192	99.58157998	0.418420016	192	99.68336979	0.316630209
113	99.36378798	0.636212021	113	98.9339472	1.066052798	193	99.58482207	0.415177929	193	99.68678211	0.313217885
114	99.36922324	0.630776757	114	98.97262815	1.027371845	194	99.58529885	0.414701151	194	99.69038534	0.309614663
115	99.3770424	0.622957604	115	99.00849334	0.991506655	195	99.58787345	0.412126552	195	99.69343972	0.306560275
116	99.38295444	0.617045562	116	99.04192457	0.95807543	196	99.59016198	0.40983802	196	99.69778268	0.302217318
117	99.38810364	0.611896364	117	99.07511717	0.92488283	197	99.59216445	0.407835554	197	99.70169612	0.298303884
118	99.39287141	0.607128588	118	99.10334639	0.896653608	198	99.59302265	0.406977354	198	99.70498913	0.295010873
119	99.39735312	0.602646878	119	99.1314563	0.868543699	199	99.5939762	0.406023799	199	99.70780489	0.292195109
120	99.40135805	0.598641947	120	99.15777653	0.84222347	200	99.59531118	0.404688822	200	99.71064452	0.289355484
121	99.40526763	0.59473237	121	99.18278433	0.817215673	201	99.59731364	0.402686356	201	99.71403298	0.285967023
122	99.40946327	0.590536728	122	99.20581154	0.794188455	202	99.59864862	0.401351378	202	99.71596583	0.284034168
123	99.41289607	0.587103929	123	99.22912511	0.770874889	203	99.59950682	0.400493179	203	99.72057128	0.279428725
124	99.4160428	0.583957197	124	99.24857297	0.751427031	204	99.60065109	0.399348913	204	99.72393587	0.276064126
125	99.41976167	0.580238332	125	99.26823559	0.731764412	205	99.60103251	0.39896749	205	99.72730047	0.272699527
126	99.42300376	0.576996244	126	99.28804138	0.711958619	206	99.60103251	0.39896749	206	99.7289947	0.271005297
127	99.425483	0.574517	127	99.30479279	0.695207213	207	99.60150929	0.398490713	207	99.73173888	0.268261121
128	99.42758082	0.572419179	128	99.32035107	0.679648927	208	99.60179535	0.398204646	208	99.73586707	0.264132925
129	99.42929722	0.57070278	129	99.33593322	0.664066778	209	99.60189071	0.398109291	209	99.73999527	0.26000473
130	99.43158575	0.568414247	130	99.35149151	0.648508493	210	99.60274891	0.397251091	210	99.74414733	0.255852672
131	99.43444642	0.565553582	131	99.36425789	0.635742108	211	99.60274891	0.397251091	211	99.74667674	0.253323257
132	99.43740244	0.562597561	132	99.37759698	0.622403025	212	99.60274891	0.397251091	212	99.74872891	0.25127109
133	99.43930955	0.56069045	133	99.39002929	0.609970714	213	99.60351175	0.396488247	213	99.75128219	0.248717813
134	99.44264699	0.557353007	134	99.40272408	0.597275916	214	99.60389318	0.396106825	214	99.75369229	0.246307711
135	99.4445541	0.555445897	135	99.41358148	0.586418523	215	99.60475137	0.395248625	215	99.75619784	0.243802159
136	99.44693799	0.553062009	136	99.42310258	0.576897425	216	99.6051328	0.394867203	216	99.75870339	0.241296607
137	99.4497033	0.550296699	137	99.43353044	0.566469555	217	99.6051328	0.394867203	217	99.76094646	0.239053541
138	99.45285003	0.547149967	138	99.44305154	0.556948457	218	99.6051328	0.394867203	218	99.76338042	0.236619576
139	99.45580605	0.544193945	139	99.45176132	0.548238868	219	99.60532351	0.394676492	219	99.76562349	0.23437651
140	99.45952492	0.54047508	140	99.46042337	0.539576628	220	99.60532351	0.394676492	220	99.76810518	0.23189482
141	99.46209952	0.537900481	141	99.46791617	0.532083834	221	99.60589564	0.394104359	221	99.7702528	0.229747204
142	99.46400663	0.535993371	142	99.47543282	0.524567178	222	99.605991	0.394009003	222	99.77185158	0.228148423
143	99.46648587	0.5335141									

228	99.605991	0.394009003	228	99.78163516	0.218364838
229	99.605991	0.394009003	229	99.7836396	0.216360397
230	99.605991	0.394009003	230	99.78480886	0.215191139
231	99.605991	0.394009003	231	99.78614516	0.213854845
232	99.605991	0.394009003	232	99.78714738	0.212852624
233	99.605991	0.394009003	233	99.78779166	0.212208339
234	99.605991	0.394009003	234	99.78855526	0.211444742
235	99.605991	0.394009003	235	99.78958134	0.210418659
236	99.605991	0.394009003	236	99.79072674	0.209273263
237	99.605991	0.394009003	237	99.79079832	0.209201676
238	99.605991	0.394009003	238	99.79282663	0.207173372
239	99.605991	0.394009003	239	99.79301753	0.206982473
240	99.605991	0.394009003	240	99.7935425	0.2064575
241	99.605991	0.394009003	241	99.79509356	0.204906444
242	99.605991	0.394009003	242	99.79509356	0.204906444
243	99.605991	0.394009003	243	99.7961435	0.203856498
244	99.605991	0.394009003	244	99.7961435	0.203856498
245	99.605991	0.394009003	245	99.79716959	0.202830415
246	99.605991	0.394009003	246	99.79757525	0.202424754
247	99.605991	0.394009003	247	99.79757525	0.202424754
248	99.605991	0.394009003	248	99.79895927	0.201040735
249	99.605991	0.394009003	249	99.79926948	0.200730524
250	99.605991	0.394009003	250	99.79926948	0.200730524
251	99.605991	0.394009003	251	99.79984217	0.200157826
252	99.605991	0.394009003	252	99.79984217	0.200157826
253	99.605991	0.394009003	253	99.8004626	0.199537403
254	99.605991	0.394009003	254	99.80084439	0.199155605
255	99.605991	0.394009003	255	99.80280111	0.197198888

Fig. 7 shows graphical presentation of the values of ToT, and HVQT of the original gold mine image of size 117x891, its zero diluted version of size 2352x1781, the reconstructed image by interpolant prediction using pixel averaging and the reconstructed image by interpolant prediction using extended morphological filtering.

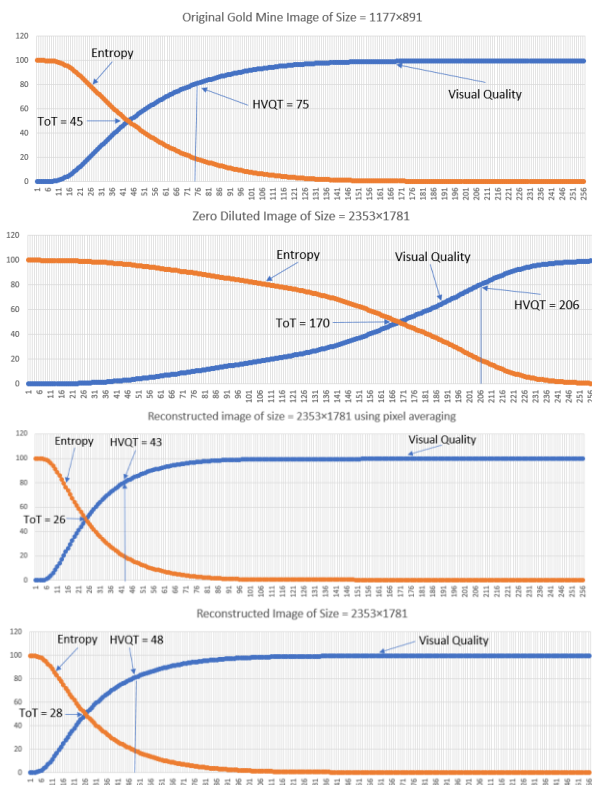


Fig. 7. Graphs of visual quality parametric values of sample image, zero diluted version and the reconstructed forms.

#### Observations

1. ToT and HVQT in zero diluted image are very poor (ie., ToT = 170 and HVQT = 206).

2. ToT and HVQT in the reconstructed image using prediction formula is pretty much closer to the original image.

3. ToT and HVQT in the reconstructed image using extended morphological filter is pretty much closer to the original image.

4. There is an increase in the contrast in the reconstructed images when compared to the original image.

### III. CONCLUSIONS

Two methods for predicting interpolant pixel values of a zero diluted image (i) interpolant prediction using neighborhood pixel value averaging and (ii) interpolant prediction using extended morphological filtering are discussed briefly in this paper with a real time sample image. While both methods yield appreciable results, interpolant prediction using extended morphological filtering seems to be better than the interpolant prediction using neighborhood averaging, in the sense of prediction accuracy.

### ACKNOWLEDGEMENT

The authors put on records the support extended by MG-NIRSA, Hyderabad, Pentagram Research Centre Pvt Ltd., Hyderabad, University of Petroleum and Energy Studies, Dehradun and Avatar MedVision US LLC, NC, USA. Thanks are due to Dr.ShankarLingam, MG-NIRSA for coordinating with University of Mysore while the first author was carrying out PhD.

#### Advisory Committee Members and Co-authors

1. Dr. Amit Agarwal, Director, APJ Abdul Kalam, Institute of Technology, Dehradun, India.
2. Dr. Michael Patrick Coyle, Chief Executive Officer, Avatar MedVision US LLC, NC, USA.
3. Sathya Govindarajan, Director, Pentagram Research Centre Private Limited, Hyderabad, India.
4. Prashanthi Govindarajan, Director, Pentagram Research Centre Private Limited, Hyderabad, India.
5. Yashaswi Vemuganti, Consultant, Avatar MedVision US LLC, NC, USA.
6. Dr. Jean Claude Perez, IBM European Research Center on Artificial Intelligence, France.
7. Dr. Hindupur Rajasimha, Chief Engineer, Indian Space Research Organization and IDBI (Retd.).

### REFERENCES

- [1] Jean Serra; Cube, cube-octahedron or rhomb-dodecahedron as bases for 3-D shape descriptions, *Advances in visual form analysis*, World Scientific 1997, 502-519.
- [2] Wuthrich, C.A. and Stucki, P.; An algorithm comparison between square- and hexagonal based grids; *Graphical Models and Image Processing*, 53(4), 324-339,1991.
- [3] Reinhard Klette and Aziel Rosenfeld; *Digital Geometry: Geometric methods for picture analysis*; Elsevier, 2004.
- [4] B. Nagy; *Geometry of Neighborhood sequences in hexagonal grid; Discrete Geometry of computer imagery*; LNCS-4245, Springer.
- [5] Tristan Roussillon, Laure Tougne, and Isabelle Sivignon; *What Does Digital Straightness tell about Digital Convexity?*.
- [6] Edward Angel, "Interactive Computer Graphics- a top down approach with OpenGL", Second Edition, Addison Wesley, 2000.
- [7] S.W. Zucker, R.A. Hummel, "A Three-Dimensional Edge Operator", *IEEE Trans. On PAMI*, Vol. 3, May 1981.

- [8] Jürgen, H., Manner, R., Knittel, G., and Strasser, W. (1995). Three Architectures for Volume Rendering. *International Journal of the Eurographics Association*, 14, 111-122.
- [9] Dachille, F. (1997). *Volume Visualization Algorithms and Architectures*. Research Proficiency Examination, SUNY at Stony Brook.
- [10] Günther, T., Poliwoda, C., Reinhart, C., Hesser, J., and Manner, J. (1994). VIRIM: A Massively Parallel Processor for Real-Time Volume Visualization in Medicine. *Proceedings of the 9th Eurographics Hardware Workshop*, 103-108.
- [11] Boer, M.De, Gröpl, A., Hesser, J., and Manner, R. (1996). Latency- and Hazard-free Volume Memory Architecture for Direct Volume Rendering. *Eurographics Workshop on Graphics Hardware*, 109-119.
- [12] Swan, J.E. (1997). *Object Order Rendering of Discrete Objects*. PhD. Thesis, Department of Computer and Information Science, The Ohio State University.
- [13] Yagel, R. (1996). *Classification and Survey of Algorithms for Volume Viewing*. SIGGRAPH tutorial notes (course 34).
- [14] Law, A. (1996). *Exploiting Coherency in Parallel Algorithms for Volume Rendering*. PhD. Thesis, Department of Computer and Information Science, The Ohio State University.
- [15] Ray, H., Pfister, H., Silver, D., and Cook, T.A. (1999). Ray Casting Architectures for Volume Visualization. *IEEE Transactions on Visualization and Computer Graphics*, 5(3), 210-233.
- [16] Yagel, R. (1996). Towards Real Time Volume Rendering. *Proceedings of GRAPHICON' 96*, 230-241.
- [17] Kaufman, A.E. (1994). Voxels as a Computational Representation of Geometry. in *The Computational Representation of Geometry SIGGRAPH '94 Course Notes*.
- [18] Lacroute, P., and Levoy, M. (1994). Fast Volume Rendering Using a Shear-Warp Factorization of the Viewing Transform. *Computer Graphics Proceedings Annual Conference Series ACM SIGGRAPH*, 451-458.
- [19] Sutherland, I.E., Sproull, R.F., and Schumaker, R.A. (1974) A Characterization of Ten Hidden Surface Algorithms. *ACM Computing Surveys*, 6(1), 1-55.
- [20] Roberts, J.C. (1993). *An Overview of Rendering from Volume Data including Surface and Volume Rendering*. Technical Report 13-93\*, University of Kent, Computing Laboratory, Canterbury, UK.
- [21] Frieder, G., Gordon, D., and Reynolds, R.A. (1985). Back-to-Front Display of Voxel-Based Objects. *IEEE Computer Graphics and Applications*, 5(1), 52-60.
- [22] Westover, A.L. (1991). *Splatting: A Parallel Feed-Forward Volume Rendering Algorithm*. Ph.D. Dissertation, Department of Computer Science, The University of North Carolina at Chapel Hill.
- [23] Zwicker, M., Pfister, H., Baar, J.B. and Gross M. (2001). Surface Splatting. In *Computer Graphics SIGGRAPH 2001 Proceedings*, 371-378.
- [24] Nulkar, M., and Mueller, K. (2001). Splatting With Shadows. *International Workshop on Volume Graphics 2001*, 35-50.
- [25] J. Krüger and R. Westermann, *Acceleration Techniques for GPU-based Volume Rendering*, *Proceedings of the 14th IEEE Visualization 2003 (VIS'03)*, 38-43.
- [26] Markus Hadwiger, Joe M. Kniss, Christ of Rezk-salama, Daniel Weiskopf, and Klaus Engel. *Real time Volume Graphics*. A. K. Peters, Ltd., USA, 2006.
- [27] Goodman, D., Nishimura, Y., Hongo, H and Noriaki N., 2006. Correcting for topography and the tilt of the GPR antenna, *Archaeological Prospection*, 13: 157-161.
- [28] Goodman, D., Y. Nishimura, and J. D. Rogers, 1995. GPR time slices in archaeological prospection: *Archaeological Prospection*, 2:85-89.
- [29] Goodman, D., 1994. Ground-penetrating radar simulation in engineering and archaeology: *GEOPHYSICS*, 59:224-232.